A dynamic region estimation method for cerebral perfusion CT

G. Van Eyndhoven[a], J. De Beenhouwer[b] and J. Sijbers[c]

Abstract

In cerebral perfusion computed tomography (PCT), multiple scans of the brain are acquired after an intravenous contrast bolus injection. Therefore, radiation dose is a major issue.

Recently, methods have been proposed that can reconstruct high quality dynamic (i.e., 4D) images, while keeping the radiation dose limited. These methods typically require an accurate estimate of the dynamic region inside the brain volume, i.e., the region containing tissue/vessels. Conventionally, the dynamic region is indicated manually.

In this work, a method for low-dose cerebral PCT is presented in which the dynamic region is estimated in an automatic way.

Simulation results on two PCT phantoms show that the dynamic region can be accurately estimated, even in a very low-dose regime, which is an important step towards more powerful reconstruction methods for low-dose cerebral PCT.

Contact information

[a] geert.vaneyndhoven@uantwerpen.be
iMinds-Vision Lab, University of Antwerp
B-2610 Antwerp, Belgium

[b] jan.debeenhouwer@uantwerpen.be
iMinds-Vision Lab, University of Antwerp
B-2610 Antwerp, Belgium

[c] jan.sijbers@uantwerpen.be
iMinds-Vision Lab, University of Antwerp
B-2610 Antwerp, Belgium

1. Introduction

Cerebral perfusion computed tomography (PCT) is an important imaging technique to detect and diagnose acute stroke events. During a stroke event, the blood supply to the brain is locally disturbed, resulting in rapid loss of brain function [1].

In PCT, a time-varying brain volume is reconstructed based on multiple scans of the brain volume after an intravenous contrast bolus injection. From the PCT scans, diagnostic relevant perfusion maps such as cerebral blood volume and cerebral blood volume can be derived [2-4]. These perfusion maps allow for identifying the extent of a region of severely ischemic but potentially salvageable brain tissue, which is important therapeutic information for the clinician.

Because the same volume needs to be scanned multiple times, radiation dose is a major issue. A straightforward solution for lowering the radiation dose consists of reducing the exposure time or the number of acquired projection images. However, if standard reconstruction algorithms such as the simultaneous iterative reconstruction technique (SIRT) [5] or filtered backprojection (FBP) [6] are utilized, this will typically lead to artifacts in the reconstructed volumes, which may result in erroneous diagnosis.

Recently, various reconstruction algorithms have been proposed that can produce adequate image quality for a lower radiation dose [7-10]. These methods typically require an accurate estimate of the dynamic region, i.e., the region containing tissue/vessels that have a time-varying attenuation coefficient due to the injected contrast agent. However, finding this region is far from trivial, especially in the case of low-dose PCT, and, to the authors' knowledge, no research has been published on how to accurately estimate this region. Therefore, the dynamic region is usually indicated manually or estimated with a simple threshold method, thereby introducing errors that propagate through the entire reconstruction/post-processing procedure.

In this work, a new dynamic region estimation method for low-dose cerebral PCT is presented. The dynamic region is automatically estimated using an optimization approach that enforces PCT-specific model restrictions on the reconstructed volume while maximizing correspondence with the projection data and minimizing model-fitting errors in the dynamic region.

In Section 2, some basic concepts of computed tomography are introduced, followed by a description of the model-specific assumptions in PCT and the dynamic region estimation method. Various validation experiments are reported in Section 3. The paper is concluded in Section 4.

2. Method

2.1 Computed tomography

The reconstructed image of the scanned object is represented on a pixel grid. The pixel values of the image are represented by a $N \times 1$ column vector $\boldsymbol{x} = (x_i) \in \mathbb{R}^N$. The scanning process results in M data values, which are log-corrected and ordered in a vector $\boldsymbol{p} = (p_i) \in \mathbb{R}^M$. We refer to $\boldsymbol{p}$ as the *projection data* or *sinogram*. Given a reconstructed image $\boldsymbol{x}$, the i^{th} projection value can be simulated by the linear combination $\sum_{j=1}^{N} w_{ij} x_j$, where w_{ij} usually represents the intersection length between pixel j and projection line i. If all the weights are properly stored into a (sparse) matrix $\boldsymbol{W} = (w_{ij}) \in \mathbb{R}^{MxN}$, the correspondence between the projection data $\boldsymbol{p}$ and the image $\boldsymbol{x}$ can be written as a system of linear equations $\boldsymbol{Wx} = \boldsymbol{p}$. Since noise and discretization effects render this system inconsistent, algebraic reconstruction methods (such as SIRT) typically minimize the

projection distance $||\boldsymbol{Wx} - \boldsymbol{p}||$ for some norm $||\cdot||$. In this work, we frequently simulate the sinogram with the forward projection operator $\boldsymbol{W}$, which was implemented using the ASTRA toolbox [11,12].

In perfusion CT, the brain volume is reconstructed on a predefined number of time points T. This is achieved by rotating the source and detector T times around the brain volume, thereby collecting T sets of projection data over the full 180° range. Conventionally, the brain volume is then reconstructed on T different time points, where each individual reconstruction is based on its corresponding full 180° angular range projection data.

2.2 Model assumptions

The dynamic region estimation method that is introduced in this paper relies on two model assumptions for cerebral PCT.

The first assumption is trivial: the time-varying brain volume consists of both stationary regions (the bone and void space) and dynamic regions (arteries and brain tissue).

Secondly, the concentration curves (i.e., the temporal evolution of the contrast agent concentration in each pixel) in the dynamic region can be described by a linear combination of time-shifted gamma variate functions, since the flow of contrast agent through a particular pixel has smooth rise and fall characteristics [13]. In this work, the gamma variate functions are defined by their simplified form

$$y(t) = (t - t_0)^{\kappa} \exp\left(-\frac{t - t_0}{\beta}\right), \tag{1}$$

where κ and β are two parameters describing the shape, and t_0 is a temporal shift. It is assumed that each TCC can be described by a linear combination of five time-shifted gamma variate functions y_1, y_2, y_3, y_4, y_5, where we have chosen $\kappa = 2$ and $\beta = 4$ for each of these curves. The parameter t_0 is chosen such as to distribute the gamma variate functions uniformly over the full time interval. The resulting gamma variate functions are shown in the left plot of Figure 1.

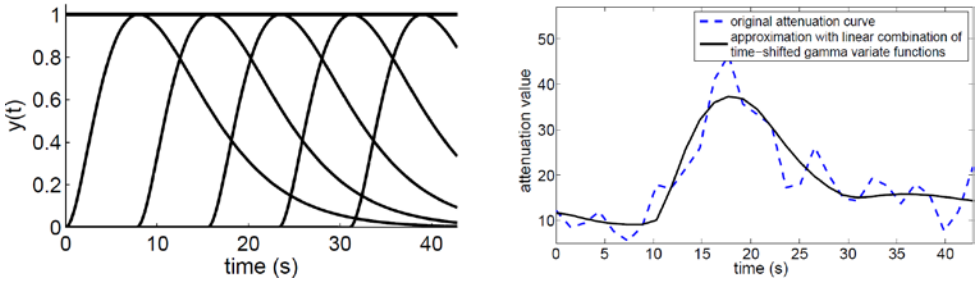

Figure 1: *Left: The 5 time-shifted gamma variate functions and the constant function. Right: A typical time attenuation curve extracted from a specific pixel in a SIRT reconstruction and its least square approximation by a linear combination of the time-shifted gamma variate functions and the constant function.*

To model the constant attenuation offset of the attenuation curves, the set of five gamma-variate functions is augmented with a sixth function $y_6 = 1$. It is now assumed that the attenuation curve of every pixel in the dynamic region can be described as

$$x(t) = \sum_{i=1}^{6} a_i y_i(t), \tag{2}$$

where *x(t)* represents the time-dependent model of attenuation in a specific pixel. In practice, this model assumption can be enforced by least squares fitting of (2) to each extracted attenuation curve. An example of such a fitted function is visualized in the right plot of Figure 1.

2.3 Dynamic region estimation method

In this section, the dynamic region estimation method is explained in detail. First, the B-spline based closed curve representation of the dynamic region is described in section 2.3.1. Next, in section 2.3.2, the objective function that quantifies the current dynamic region estimation quality is introduced. Finally, the minimization procedure is explained in section 2.3.3.

2.3.1 Dynamic region descriptor

A brief description of the parametric B-spline closed curve model [14,15] for representing the dynamic region is given. To define the normalized B-spline closed curve of degree k with n control points, we first introduce $n + 2k + 1$ knot-points $t_{-k} < t_{-k+1} < \ldots < t_{n+k} \in \mathbb{R}$. The following recursion relations are used to define the normalized B-spline basis functions of degree k for $i = -k, -k+1, \ldots, n-1$:

$$N_{i,k+1}(t) = \frac{t - t_i}{t_{i+k} - t_i} N_{i,k}(t) + \frac{t_{i+k+1} - t}{t_{i+k+1} - t_{i+1}} N_{i+1,k}(t) \tag{3}$$

$$N_{i,1}(t) = \begin{cases} 1 & \text{if} \quad t_i \le t < t_{i+1} \\ 0 & \text{otherwise} \end{cases} \tag{4}$$

These B-spline basis functions allow us to define the closed curve $\boldsymbol{c}(t)$ with $t \in [t_0, t_n]$ being the parameter describing the exact location on the curve:

$$\boldsymbol{c}(t) = \sum_{i=-k}^{n-1} \boldsymbol{c}_i N_{i,k+1}(t) \tag{5}$$

The vectors $\boldsymbol{c}_i \in \mathbb{R}^2$ are the control points and are chosen such that $\boldsymbol{c}_i = \boldsymbol{c}_{i-n}$ for $i = n-k, \ldots, n-1$. Once the knot-points $t_{-k} < t_{-k+1} < \ldots < t_{n+k}$ are fixed, the region within the closed curve $\boldsymbol{c}$ is completely described by the coordinates of the control point $\boldsymbol{c}_0, \boldsymbol{c}_1, \ldots, \boldsymbol{c}_{n-1}$. As an example, a B-spline based closed curve of degree *k=2* and with *n=10* control points is visualized in Figure 2.

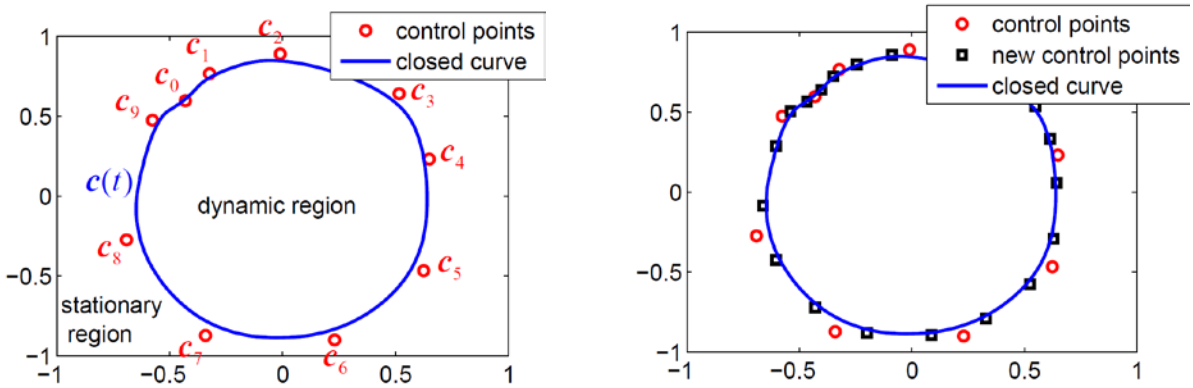

Figure 2: *Left: A B-spline based closed curve of degree k=2 and with n=10 control points* $\boldsymbol{c}_0, \boldsymbol{c}_1, \ldots, \boldsymbol{c}_9$. *Right: The same closed curve c(t) represented with twice the amount of control points.*

A useful property of the B-spline based closed curve is the fact that the same closed curve can be easily represented by twice the number of spline control points by applying Boehm's formula for knot insertion [15]. This is also visualized in Figure 2. This property is exploited to implement a multiresolution minimization approach, described in section 2.3.3.

2.3.2 Objective function

For every possible set of control points that represent an estimate of the dynamic region, an objective function value is calculated, quantifying the quality of the dynamic region estimation. The coordinates of the B-spline closed curve control points are ordered in a parameter vector $\boldsymbol{\alpha}$, describing the degrees of freedom of our optimization routine. All steps for evaluating the objective function are visualized in Figure 3.

The objective function is based on the measured projection data and a preliminary reconstruction, which can for example be calculated with SIRT or FBP. The objective function is formed by a weighted sum of two terms: A model-based projection distance (MPD) term and a model-fit error correlation measure (MEC).

The MPD term quantifies how likely the current dynamic region estimate $\boldsymbol{\alpha}$ is to occur by inferring model assumptions back to the originally measured data, i.e., the measured sinogram. To calculate the MPD term, the attenuation curves of the preliminary reconstruction are replaced by their mean in the current stationary region (i.e., the dynamic region's complement) and by the attenuation curve's least squares approximation based on a linear combination of time-shifted gamma variate basis functions and the constant function (Section 2.2, equation (2)) in the dynamic region. This modification forces the reconstruction to adhere to the model assumptions that were introduced in section 2.2. If the current dynamic region estimate $\boldsymbol{\alpha}$ is far from the true dynamic region, this step will introduce large errors. If the current estimate $\boldsymbol{\alpha}$ close to the true dynamic region, this processing step will improve the preliminary reconstruction. Next, a simulated sinogram is calculated by forward projecting the processed reconstruction. This simulated sinogram is compared to the measured sinogram by calculating the sum of squared differences, normalized with the energy in the measured sinogram:

$$MPD = \frac{\sum_{i=1}^{M} (p_{sim}(i) - p_{meas}(i))^2}{\sum_{i=1}^{M} (p_{meas}(i))^2}, \tag{6}$$

where M is the number of measured sinogram values and p_{sim} and p_{meas} are the simulated and measured sinogram, respectively. Errors in the dynamic region's estimate $\boldsymbol{\alpha}$ will introduce large errors in the processed reconstruction. This will propagate towards a mismatch between the simulated sinogram and the measured sinogram, resulting in a higher MPD. An accurate estimate $\boldsymbol{\alpha}$ results in a simulated sinogram closely related to the measured sinogram and hence a lower MPD.

The MEC term quantifies how well the linear combination of time-shifted gamma variate basis functions describes the time concentration curves in the dynamic region. The first step consists of calculating the linear combination of the 5 time-shifted gamma variate function and the constant function (see Section 2.2) to approximate the time attenuation curve of each pixel in the dynamic region. After subtracting the constant function, the time concentration curves are obtained, as is illustrated on the flowchart in Figure 3. If the time concentration curve is close to a constant

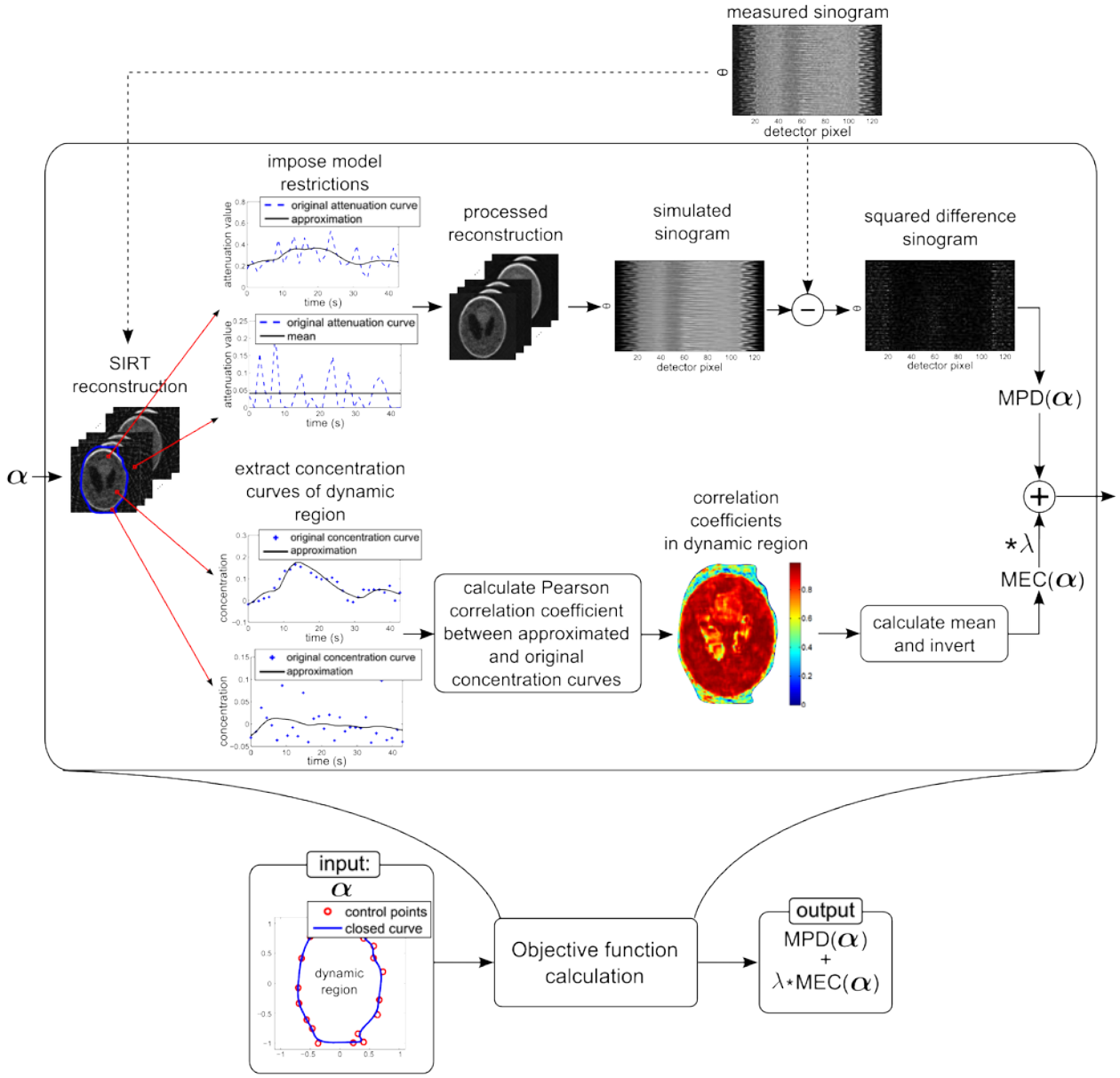

Figure 3: *Flowchart for calculating the objective function value*

function around zero, the correlation between the fitted and the original concentration curve will be low. However, if the concentration curve exhibits rise and fall characteristics, the approximation with time-shifted gamma variate functions will be highly correlated with the original concentration curve. Therefore, the Pearson correlation coefficient between the original and the approximated concentration curve is calculated:

$$r_{f_1 f_2} = \frac{\sum_{i=1}^{T}(f_1(i)-\overline{f_1})(f_2(i)-\overline{f_2})}{\sqrt{\sum_{i=1}^{T}(f_1(i)-\overline{f_1})}\sqrt{\sum_{i=1}^{T}(f_2(i)-\overline{f_2})}}, \quad (7)$$

where T represents the number of time points and f_1 and f_2 represent the discrete representations of the approximated and the original concentration curve. This Pearson correlation coefficient is calculated for each pixel in the dynamic region, as is illustrated in the flowchart of Figure 3. Finally, MEC is defined as the inverse of the mean of the Pearson correlation coefficients over all dynamic pixels. This will be higher if the dynamic region estimate is overestimated (i.e., it also includes stationary pixels) and will be lower if less stationary pixels are included in the dynamic region's estimate.

The objective function value is formed by the weighted sum $MPD(\boldsymbol{\alpha}) + \lambda * MEC(\boldsymbol{\alpha})$, where λ controls the trade-off between these two terms. The objective function's behavior is evaluated in more detail in Section 3.2.

2.3.3 Minimization

The minimization procedure starts from an initial estimate calculated with a basic method as follows. First, a standard SIRT reconstruction is filtered with a three-dimensional $3 \times 3 \times 3$ averaging filter. Next, the corresponding concentration curves are thresholded to produce a binary image. From this binary image mask, the largest connected component is selected and its holes are filled. This method for calculating the dynamic region is referred to as the *basic method*. Finally, the initial parameter vector $\boldsymbol{\alpha}_0$ is obtained by approximating the edge of the basic estimate with a B-spline based closed curve.

Starting from the initial parameter vector $\boldsymbol{\alpha}_0$, the minimization is performed with a multiresolution approach that starts at level $L=3$ and proceeds as follows:

1. Calculate a SIRT reconstruction on T/L time points by joining every subsequent L projection datasets and applying SIRT on the joined projection datasets. This will introduce more motion artifacts in the reconstruction (due to the fact that the reconstruction was based on inconsistent projection data) but will reduce noise and limited data artifacts. Apply a block matching filter to this SIRT reconstruction, to further reduce the influence of the noise [16]. The obtained reconstruction is further utilized in the calculation of the objective function in step 2.
2. Loop over each control point and move it away and towards the center of mass of the current dynamic region's estimate. This is illustrated for one control point in Figure 5. For each position, calculate the objective function value and finally change the control point towards the position with the lowest objective function value.
3. If the current level L=1, the minimization procedure is finished. Otherwise, double the number of control points, set L = L-1 and go back to step 1.

3. Experiments

3.1 Phantoms

The two simulation phantoms that were utilized in this paper are visualized in Figure 4. The Shepp-Logan phantom was modified by superimposing various concentration curves that represent different types of tissue. The brain phantom was taken from literature and represents a more realistic PCT phantom [17-18]. Each of the phantoms were defined on a 256×256 pixel grid and simulated on 30 points in time. The projections were simulated with a strip kernel and Poisson distributed noise was applied to the projections [6]. The reconstructions were calculated on a 128×128 pixel grid. As a validation measure, the number of misclassified pixels (NMP) is utilized. It is defined as the number of pixels that are misclassified with respect to the ground

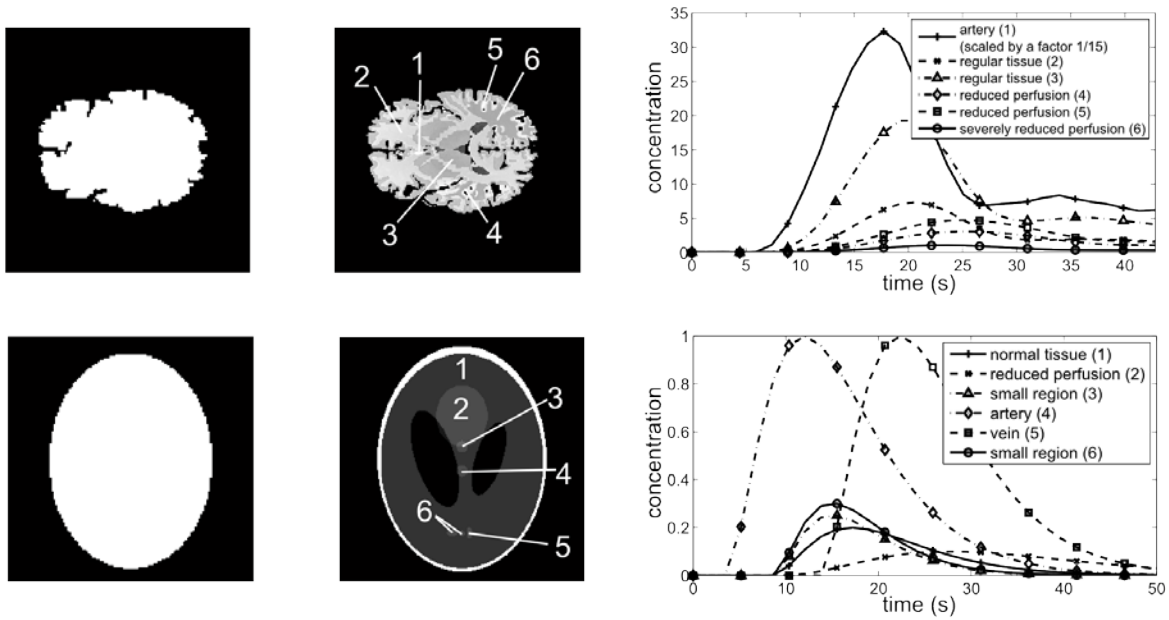

Figure 4: *The two simulation phantoms. The top row represents the digital brain phantom, the bottom row the modified Shepp-Logan phantom. First column: the ground truth dynamic region. Second column: The phantom at the first time point. Last column: The concentration curves for different types of pixels.*

truth dynamic region mask. In all our experiments, the initial number of control points was set to 20 and the weighting parameter λ was set to 0.03.

3.2 Objective function's behavior

The objective function's behavior is illustrated in Figure 5.

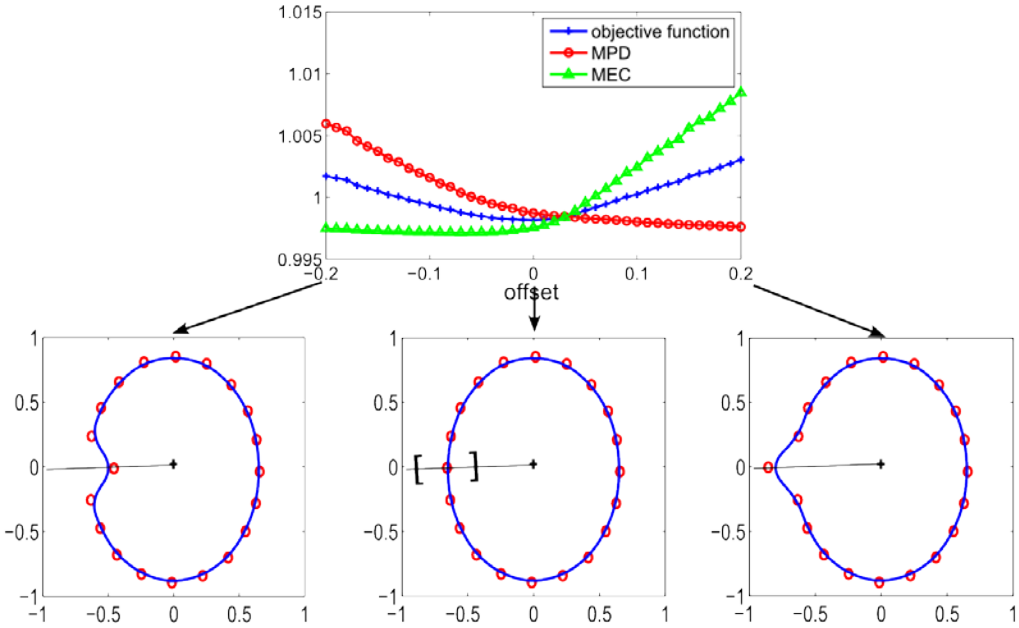

Figure 5: *Illustration of the objective function's behavior. The x-axis corresponds to the offset of the indicated control point in the direction towards or away from the center of mass of the dynamic region. The central dynamic region image corresponds to the ground truth for the Shepp-Logan experiment. The objective function value, MEC and MPD term were scaled to be able to represent them on the same plot.*

For this experiment, 20 projections were simulated for each of the 30 time points of the modified Shepp-Logan phantom. Starting from the ground truth dynamic region (indicated by offset 0 in Figure 5), the indicated control point was moved towards and away from the dynamic region's center of mass. The MPD, MEC and objective function value (scaled such that they can be visualized in the same plot) were calculated for each position of that particular control point. From Figure 5, it can be seen that the ground truth dynamic region corresponds to minimum of the objective function, and that changing the ground truth dynamic region will increase the objective function value.

3.3 Region estimation quality

In a first experiment, a total of 600 projections were simulated (corresponding to 10 projections per time point) for both the Shepp-Logan and the digital brain phantom. The result of the basic and the proposed method are visualized in Figure 6.

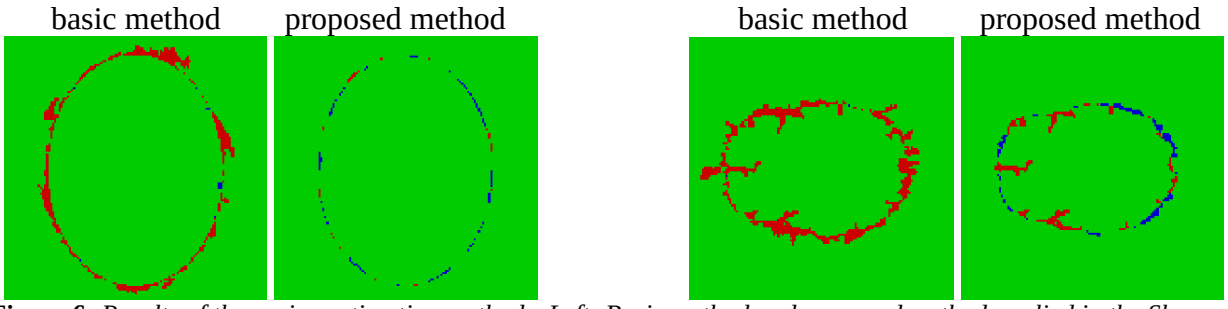

Figure 6: *Results of the region estimation methods. Left: Basic method and proposed method applied in the Shepp-Logan experiment. Right: Basic method and proposed method applied in the digital brain experiment. The pixels are color-coded as follows: Green refers to correctly classified pixels, red refers to pixels that were misclassified as dynamic and blue refers to pixels that were misclassified as stationary.*

The previous experiment was repeated several times, each time for a different number of simulated projections per time point. For each of these set-ups, the NMP was calculated and plotted in function of the simulated number of projections per time point in Figure 7.

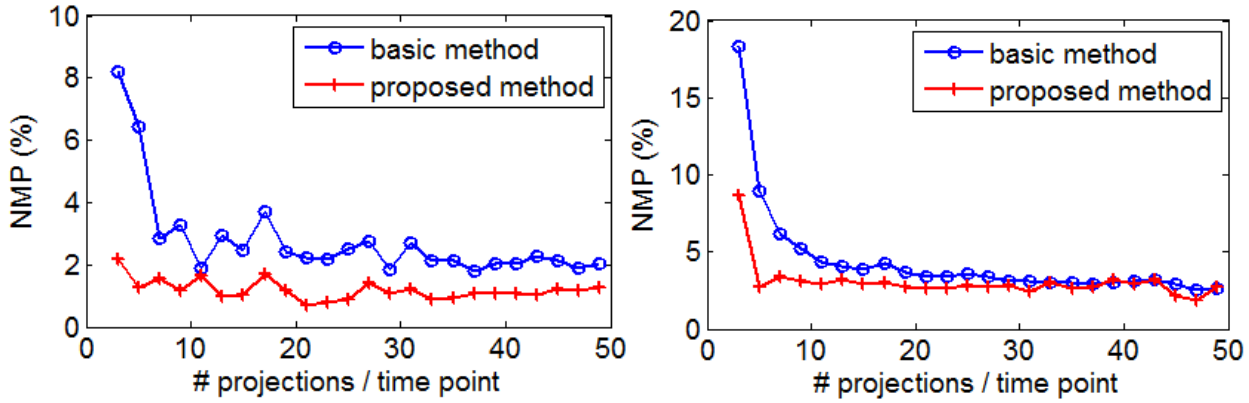

Figure 7: *The NMP in function of the number of projections per time frame for both the proposed region estimation method and the basic method. The left plot is for the Shepp-Logan phantom and the right plot for the digital brain perfusion phantom.*

4. Conclusions

We presented a robust dynamic region estimation method for PCT. Both qualitative and quantitative phantom validation experiments confirm that the proposed method can accurately estimate the dynamic region, even if only few projections are available per time point. The dynamic region's estimate can be utilized as prior knowledge in various recently proposed PCT reconstruction methods that allow for dose reduction without compromising image quality.

References

[1] K. A. Miles and M. R. Griffiths, Brit. J. Radiol., vol. 76, no. 904, pp. 220–231, 2003

[2] B. D. Murphy, A. J. Fox, D. H. Lee, D. J. Sahlas, S. E. Black, M. J. Hogan, S. B. Coutts, A. M. Demchuk, M. Goyal, R. I. Aviv, S. Symons, I. B. Gulka, V. Beletsky, D. Pelz, V. Hachinski, R. Chan, and T. Y. Lee, Stroke, vol. 37, no. 7, pp. 1771–1777, 2006.

[3] A. A. Konstas, G. V. Goldmakher, T.-Y. Lee, and M. H. Lev, Am. J. Neuroradiol., vol. 30, no. 4, pp. 662–8, 2009.

[4] A. A. Konstas, G. V. Goldmakher, T.-Y. Lee, and M. H. Lev, Am. J. Neuroradiol., vol. 30, no. 5, pp. 885–92, 2009.

[5] J. Gregor and T. Benson, IEEE Trans. Med. Imag., vol. 27, no. 7, pp. 918–24, 2008.

[6] A. C. Kak and M. Slaney, Principles of computerized tomographic imaging. Society of Industrial and Applied Mathematics, 2001.

[7] J. C. Ramirez-Giraldo, J. Trzasko, S. Leng, L. Yu, a. Manduca, and C. H. McCollough, Med. Phys., vol. 38, no. 4, p. 2157, 2011

[8] M. T. Manhart, M. Kowarschik, A. Fieselmann, Y. Deuerling-Zheng, K. Royalty, A. K. Maier, and J. Hornegger, IEEE Trans. Med. Imag., vol. 32, no. 7, pp. 1336–1348, 2013

[9] C. Neukirchen, M. Giordano, and S. Wiesner, Med. Phys., vol. 37, no. 12, p. 6125, 2010

[10] G. Van Eyndhoven, K. J. Batenburg, and J. Sijbers, IEEE Trans. Imag. Proc., vol. 23, no. 2, pp. 909–919, 2014

[11] W. J. Palenstijn, K. J. Batenburg, and J. Sijbers, J. Struct. Biol., vol. 176, no. 2, pp. 250 – 253, 2011

[12] W. J. Palenstijn, K. J. Batenburg, and J. Sijbers, in 13th Int. Conf. on Comput. and Math. Meth. in Sci. and Eng. CMMSE, 2013

[13] M. D. Harpen and M. L. Lecklitner, Med. Phys., vol. 11, p. 690, 1984

[14] C. D. Boor, J. Approx. Theory, vol. 62, pp. 50–62, 1972

317 [15] W. Boehm, Comput.-Aided. Des., vol. 12, no. 4, pp. 199–201, Jul. 1980

318 [16] M. Maggioni, V. Katkovnik, K. Egiazarian, and A. Foi, IEEE Trans. Imag. Proc., vol. 22,
319 no. 1, pp. 119–133, Jan 2013

320 [17] M. T. Manhart, M. Kowarschik, A. Fieselmann, Y. Deuerling-Zheng, K. Royalty, A. K.
321 Maier, and J. Hornegger, IEEE Trans. Med. Imag., vol. 32, no. 7, pp. 1336–1348, 2013.

322 [18] A. J. Riordan, M. Prokop, M. A. Viergever, J. W. Dankbaar, E. J. Smit, and H. W. A. M.
323 de Jong," Med. Phys., vol. 38, no. 6, pp. 3212–21, 2011.